Penerbit Akademia Baru

CFD Letters

Journal homepage: www.akademiabaru.com/cfdl.html
ISSN: 2180-1363

Effect of Peak Temperature on SAC Nano-Reinforced Fillet Height

Open Access

Muhamed Abdul Fatah Muhamed Mukhtar[1], Mohamad Aizat Abas[2,*], Fakhrozi Che Ani[3], Ahmad Amrul Muhaimin Azaman[4]

[1] Faculty of Engineering, DRB-HICOM University of Automotive Malaysia, 26607, Pekan, Pahang, Malaysia
[2] School of Mechanical Engineering, Universiti Sains Malaysia, Engineering Campus, Nibong Tebal, 14300, Penang, Malaysia
[3] Western Digital, MK13, Plot 301A Persiaran Cassia Selatan 1 Taman Perindustrian, Batu Kawan, 14100, Penang, Malaysia
[4] Faculty of Engineering, DRB-HICOM University of Automotive Malaysia, 26607, Pekan, Pahang, Malaysia

ARTICLE INFO

Article history:
Received 23 July 2020
Received in revised form 21 September 2020
Accepted 24 September 2020
Available online 30 September 2020

Keywords:
Nano-reinforced solder; SAC fillet height; nanoparticles distribution; discrete phase model; nanocomposite solder paste

ABSTRACT

Recently, the addition of new materials into the conventional solder pastes provides a viable solution to optimize the material characteristics and properties of the nano-particle filled solder paste. Addition of titanium oxide (TiO2) nanoparticles shown that it can enable better performance of the solder. However, actual industry experiment in terms of its optimum thermal profile for improved strength through good spread of nano-particles in the solder is very costly and lengthy to set up. Hence, this paper presents a preliminary study of the interaction between two models of numerical simulation namely volume of fluid (VOF) and discrete phase model (DPM) then compare with previous experimental data. This paper aims to analyse the effect of peak temperature towards the fillet height of ultra-fine Sn-Ag-Cu (SAC) solder joints doped with TiO_2 nanoparticles in an electronic assembly. For the purpose of this research, the weight percentage of the nanoparticles TiO_2 with the SAC305 lead-free reinforced solder is varied at different peak temperature and investigated in terms of particles distribution, fillet height and thermal strain. This paper presents a 3D numerical simulation of nano-reinforced lead (Pb)-free solder at the ultra-fine joint component for 01005 capacitor with dimension of 0.2 x 0.2 x 0.4 mm^3. The results obtained are confirmed by conducting an experiment using a field emission scanning electron microscope (SEM) joined with an EDS and X-ray diffraction machine. This study concludes that the best fillet height would be obtained at 250°C. The distributions of nanoparticles with 0.01 wt%, 0.05 wt%, and 0.15 wt% of weighted percentage are effectively observed by using the HRTEM analysis. Based on the study, higher temperature of the wetting region that range between 240°C and 255°C results in better particle distributions, and fillet height of the solder by using temperature in that range meets the requirement of IPC standards.

* *Corresponding author.*
E-mail address: aizatabas@usm.my (Mohamad Aizat Abas)

https://doi.org/10.37934/cfdl.12.9.91103

1. Introduction

1.1 Overview

Nowadays, the use of electronic components has extended into various functions and can be used in various devices. These components are usually small in size and are joined using soldering method. This method has become crucial in assembling the components whereby the soldering materials provide thermal, electrical, and mechanical continuity in the electronic assemblies [1]. While the conventional filler metal can be used to achieve a sound joint for certain optical components, its soldering temperature is too high to ensure dimensional stability. High soldering temperatures can degrade the properties of optical fibres and other optoelectronics such as lasers, light emitting devices (LEDs), photodetectors, or waveguide devices. In recent times, the soldering materials are added with certain types of nanoparticles that help to improve the performance and dependability of the components [2]. According to Haslinda *et al.,* [3], the inclusion of TiO_2 nanoparticles to SAC solders is comprehensively discussed in earlier research.

Among the reinforced elements introduced is TiO2 which is proved to enable better performance of the solder [3]. By adding new materials into the solder, concerns relating to thermo-mechanical stresses (CTE- coefficient of expansion) of solder, substrate and component surfaces since it started to affect the reliability of the component [3]. Based on the study by Tsao and Chang [4], the use of TiO2 nanoparticles as a supplement to the lead-free SAC mixture has significantly improved the micro-hardness of the composite solder. The use of nano-reinforced particles as supplement in the SAC305-TiO_2 nano-reinforced lead-free has greatly contributed to the increasing in strength of the solder particularly the yield stress, ultimate tensile strength, and shear strength during the micro-hardness test [4]. Tsao *et al.,* [4,5] revealed that addition of TiO_2 and Al_2O_3 nanoparticles are helpful in enhancing the overall strength of the eutectic solder [5].

1.2 Nano-Reinforced Particles as Supplement to SAC-305

According to a study by Chellvarajoo *et al.,* [6], the group used iron nickel oxide as the supplement to the SAC-305. 0.5, 1.5, and 2.5 wt% of Fe_2NiO_4 nanoparticles was mechanically added respectively to the SAC-305. The migration of nanoparticles in the nanocomposite solder paste to the outermost surface was clarified using the copper 'sandwich' method, which was performed after the reflow soldering process. Varying amounts of nanoparticles in the SAC-305 affected the IMC thickness and mechanical properties of the nanocomposite solder paste. The IMC thickness was reduced by 29.15%, 42.37%, and 59.00% after adding 0.5, 1.5, and 2.5 wt% of Fe_2NiO_4 nanoparticles in the SAC-305, respectively.

Another study by Chellvarajoo *et al.,* [7] was done by using only nickel oxide (NiO) nanoparticles as enhancement material. In the study, Sn–Ag–Cu (SAC) 305 solder alloys were mixed with 0.5, 1.5, and 2.5 wt.% NiO ceramic nano-elements to produce a new set of nanocomposite solder pastes. The displacement phenomenon of NiO nanoparticles during reflow soldering process may contribute efficient idea in the field of microelectronic industries. The reinforcement of reactive nanoparticles in SAC 305 solder paste caused 50% changes in the intermetallic (IMC) layer thickness and hardness of plain solder.

Furthermore, wetting time of the wetted solder increases and is in line with the weight percentage. Studies have shown that the discrete phase method (DPM) can be successfully used to trace the dispersion of particles [8-13].

It is apparent that temperature can be the main cause of solder joint failure mode. At room temperature, the strength of hard and brittle IMC layer is lower than the SAC305 bulk solder [14].

Temperature, which has affected the mechanical properties of the solder joint, causes a reduction in bulk solder's strength in comparison to the IMC layer. As a result, the crack propagates from IMC to bulk solder during temperature-vibration test [15]. The temperature of the soldering process typically has a greater value compared to the melting temperature. High processing temperature has been found capable of harming the electronic parts as there is a high chance that it will melt the inner solder connections[16] .

Thermal shock has a much faster ramp rate, thus imposing much more damage to the solder joints than thermal cycling. In that sense, the fatigue life decreased when the frequency increased. However, a longer dwell time causes more creep in the solder joint, thereby lowering the fatigue life significantly. This means that fatigue life decreases when frequency decreases[17]. The structure of the wetting temperature and temperature profile give effect to the structure of the solder. It is obvious that the style of temperature profile has a great effect on the reliability of solder fatigue life. The longer dwell time and the steeper ramp, the shorter the fatigue life of solder joints. This is shown in Figure 1 that as the ramp time decreases while the cycling time is kept constant, the accumulated inelastic energy density increases.

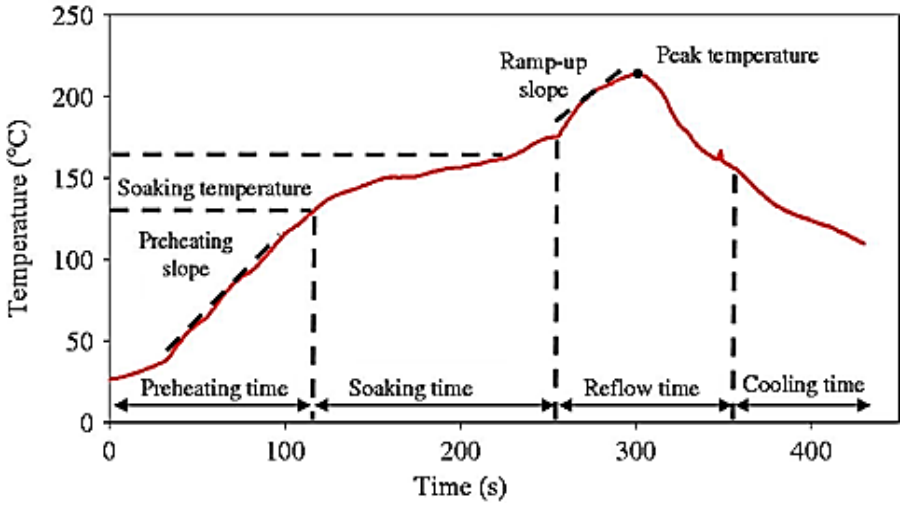

Fig. 1. Reflow Oven Thermal Profile

The computational model developed based on the reflow thermal profile of nano-reinforced lead-free solder as the wetting zone temperature between 217 °C–239 °C since this is the crucial zone in which the wetting reaction takes place on the nano-reinforced lead-free solder paste.

Taking the real measurement of the reflow oven into consideration, the mesh model is built according to the environment real size for the computer-generated soldering process of 01005 capacitors. Figure 2 shows a real size FR4-printed circuit board (PCB) with 2.0 mm thick manufactured using an organic solder-ability preservative surface finish and an ultra-fine 01005 capacitors outline that are attached on the PCB.

Even though various experimental studies have been conducted on the reinforced lead-free solder and the formation of IMC layer, limited studies have been concerted for the peak temperature effect on the IMC layer particles tracking using numerical simulation. Additionally, due to the restriction in micro-level study that includes cost and time-consuming experimental method, the need for numerical simulation that be achieved through discrete phase model (DPM) with the capability to track particle trajectory becomes indispensable. This study is focused on the impact of peak temperature to SAC nano-reinforced fillet height. Numerical simulation methods were utilized to determine the optimum pinnacle temperature of the wetting area for nano-reinforced lead-free

solder. This project includes the study method of discrete particle method (DPM) to obtain distributions of particles and the effect peak temperature thermal stress on the IMC layer. Discrete Particle Method (DPM) and Volume of Fluid (VOF) model is created and worked in a 2 ways interaction to simulate the nanoparticle distribution in the solder joint of the passive device during the soldering process.

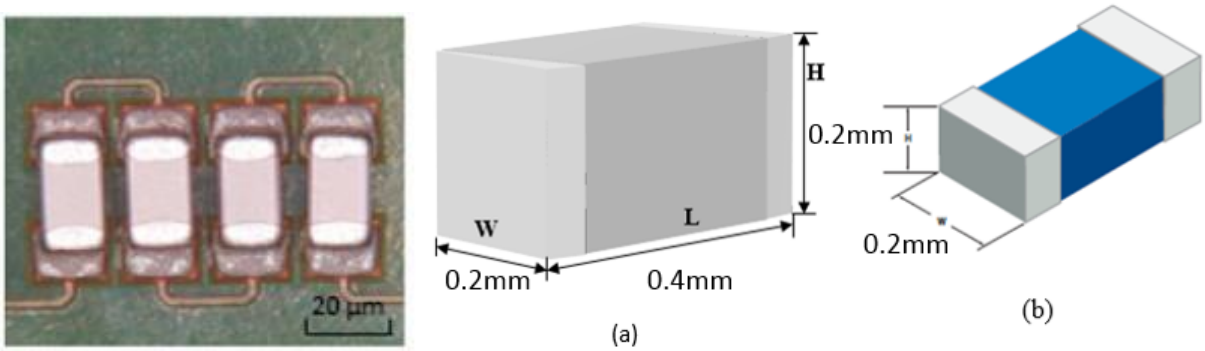

Fig. 2. FR4-printed circuit board (PCB) and outline of 01005 capacitor model

2. Methodology

2.1 Mathematical Simulation

Moving forward to the mathematical simulation of three-dimensional model of the capacitor, to mimic the atmosphere of reflow oven, the method applied is finite volume method (FVM) and it is solved by using multiphase and two Eulerian phases involved. For the wetting process of nano-reinforced lead-free solder, volume of fluid (VOF) is used while the movement of particles inside the solder is explained by using dispersed phase method (DPM). In order to simulate the real soldering solution, Table 1, Table 2, and Table 3 show the properties of SAC305 lead-free solder paste nano-reinforced, titanium oxide (TiO_2) and the IMC layer correspond to each material. The nano-sized particles are fixed inside the molten solder during the two-ways interaction of simulation between continuous phase (molten solder) and discrete phase (nano-particles).

Table 1
Properties of SAC305 lead-free solder paste

Properties	SAC305	
Density, ρ	7380	kg/m^3
Specific Heat Capacity, C_p	230	J kg ₭
Thermal Conductivity	58	Wm/K
Viscosity	0.002	kg/ms
Standard State Enthalpy	0.04	J/mol

Table 2
Properties of nano-reinforced TiO_2

Properties	TiO_2	
Density, ρ	4250	kg/m^3
Specific Heat Capacity, C_p	686	J kg ₭
Thermal Conductivity	8.95	Wm/K
Diameter, d	≈20	nm

Table 3
Cu_6Sn_5 material properties

Properties	Cu_6Sn_5		Cu_3Sn		Ni_3Sn_4	
Density, ρ	8280	kg/m^3	8900	kg/m^3	8650	kg/m^3
Specific Heat Capacity, C_p	16	J kg ₭	18	J kg ₭	15	J kg ₭
Thermal Conductivity	34.2	Wm/K	69.8	Wm/K	19.6	Wm/K
Young Modulus	85.56	GPa	108.3	GPa	133.3	GPa
Poisson's Ratio	0.309		0.299		0.330	

2.2 Grid Independent Test

By using the FVM Ansys Workbench, mesh independent analysis is performed on three-dimensional model to identify the best and suitable mesh grid resolution for a precise outcome of computational simulation. Table 4 displays the generated computational mesh of the domain in the developed model that contains ultra-fine 01005 capacitor (structure) and the solder (fluid) domain. The meshed grid with diverse medium resolutions and fine were applied in the independent grid analysis portrayed in Figure 3 and the Figure 4 shows the mesh independent grid analysis graph for Mesh Model 1-5.

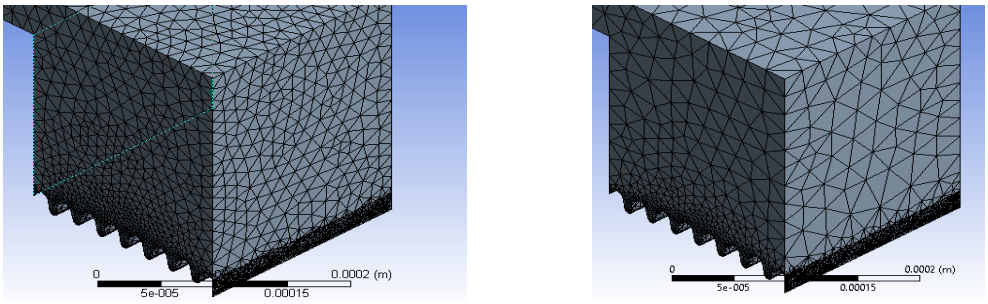

Fine mesh Medium mesh

Fig. 3. Fine mesh and medium mesh

Based on the analysis, the mesh with fine resolution and discretization error below 5% regular limits is identified as the ideal mesh because it matched perfectly with the simulation model. As can be referred from Table 1, the fine mesh model with 15281 number of nodes and 69129 number of elements is more suitable given that they enhance both computation and precision time of the acquired solution.

Table 4
Mesh independent analysis

Mesh model	Grid Resolution	Number of nodes	Number of elements	Max thermal strain (Pa)
1	Coarse	5671	22868	0.0031687
2	Medium	8642	36934	0.0035214
3	Fine	15281	69129	0.0045999
4	Fine	16025	69856	0.0046154
5	Fine	16142	70761	0.0046111

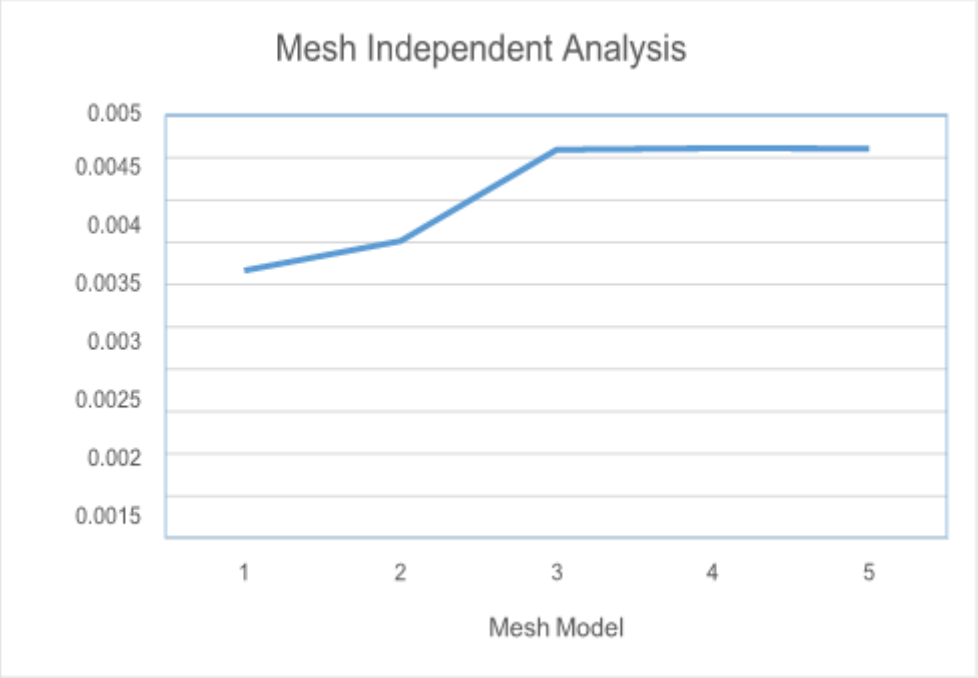

Fig. 4. Mesh independent analysis graph

2.3 Mathematical Model and Governing Equations

For three-dimensional simulation of 01005 capacitor with nano-reinforced solder, the utilization of two-way interaction involving the discrete particle phase flow and the Eulerian continuous phase flow are implemented. To numerically calculate the continuous flow of the molten wetting solder, Navier Stokes equation which consists of Eq. (1) continuity, Eq. (2) energy and Eq. (3) momentum is applied as shown below

Continuity equation

$$\frac{\partial p}{\partial t} + \nabla.(\rho\vec{u}) = 0 \tag{1}$$

Energy equation

$$\rho C_p \left(\frac{\partial T}{\partial t} + \vec{u}\nabla T\right) = \nabla(k\nabla T) + \Phi \tag{2}$$

Momentum equation

$$\frac{\partial y}{\partial x}(\rho\vec{u}) + \nabla.(\rho\vec{u}\vec{u}) = -\nabla P + \nabla.\tau + \rho\vec{g} \tag{3}$$

where,
ρ is the fluid density,
u is the velocity,
τ is the shear stress and,
g = −9.81 m/s represents gravity

The multi-phase model of the continuous phase, utilizing two Eulerian phases will be worked out with the involvement of air as the main and SAC305 as the secondary phase. The interface of both phases is related to the coefficient of surface stress. As far as the fluid domain and the base metal is concerned, the molten solder has an interfacial stress with these elements. In this research, the SAC lead-free solder, Sn-3.0Ag-0.5Cu (SAC305) with coefficients of surface stress, σ at 0.54 n/m.

Young's equation: γ SG = γ LS + γ LG cos θ

where,
γLG – σ value for liquid−gas boundary
γSG – σ value for solid−gas boundary
γLS – σ value for liquid−solid boundary
θ – contact angle

In the computational fluid dynamic (CFD) simulation, in order to trace the free surface flow for the molten solder and air interaction, the adaptation of volume of fluid (VOF) method is applied. CFD simulation with VOF model shows a good alternative to study the flowability of lead-free solder [18]. The volume fraction will be used to differentiate a varied phase that differs between 0 and 1. The volume of fluid Eq. (4) is denoted as

VOF equation

$$\frac{\partial \rho}{\partial t} f + \vec{u}.\nabla f = 0 \tag{4}$$

where f is the fraction of volume of fluid. The molten solder area is represented as 1 as it is primarily patched in the simulation.

2.4 Discrete Particle Phase Formulation

Discrete phase method (DPM) is applied to trace the change in position of the nano-reinforced TiO2 particles injected into the molten solder. The nanoparticles are being spread throughout the molten solder and realising that, two-way interaction between the continuous and discrete phase need to undergo the simulation. For continuous phase, the Eulerian model is successfully explained. Discrete phase is on the other hand, the equations represented are solver on a Langrangian frame. This is due to the particle inertia that is linked with particle force balance, Eq. (5) and the other forces as shown below

Particle force balance equation

$$\frac{\partial u_p}{\partial t} = F_D\left(u - u_p\right) + g_x \frac{(\rho_p - \rho)}{\rho_p} + F_x \tag{5}$$

2.5 Boundary Condition

For different thermal profile being used, an analysis is perfomed to examine the distribution of particle inside the molten solder after the reflow oven process. Originally, 5 mil of molten solder is mended into the model's mesh grid. The boundary condition for both capacitor and PCB is designated

as no-slip boundary and reflect [19]. Because of the motion of the molten solder (continuous phase), uniform change in momentum, of the nano-particles will be reflected at the boundary. The barriers of the component and PCB are given as reflects and no slip boundary condition. Meanwhile, the other nanoparticles will be reserved within the area of the wall [20]. In this research, the nanoparticles movement is found to be frequently affected by the motion of the molten solder. In a research carried out by F.C. Ng *et al.,* [21], the lumps of particle formed at the solder ball is identified to be the direct result of constant collision between the particles and solder balls.

As for the boundary conditions, no-slip boundary condition will be set to the wall. As far as the wetting stage is concerned, the manipulation of contact angle's setting and wall adhesion are needed and it will be set as compulsory with the surface tension value of 0.54 n/m [22]. The reflect boundary is applied for two walls that are in contact with the molten solder. Also, the interaction between the particles can be ignored either if the nano-reinforced lead free solder is smaller in size or the volume of injected particles is below 1% or combination of both. The schematic diagram of boundary condition is portrayed in Figure 5. In addition, total boundary condition is presented as Eq. 6 shown below

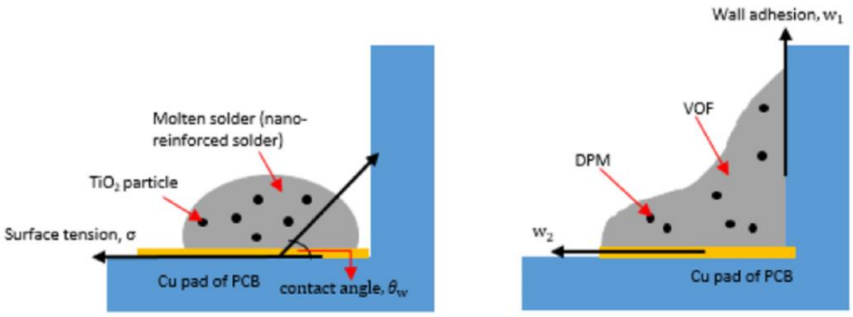

Fig. 5. Schematic diagram of boundary condition

Molten solder, fluid VOF=1, On wall, u=v=w=0;T=T_{wall};

$$\frac{\partial p}{\partial n}=0\frac{\partial p}{\partial n}=0 \tag{6}$$

On flow front : $P=P_{atn}-\frac{\sigma}{R}=P_{atn}-\frac{2\sigma\cos\vartheta}{h}$

DPM velocity, $u_p=0$

3. Results

3.1 Validation of Experimental with Simulation

From Figure 6, it can be deduced that the simulation results obtained matched the experimental results by the study of Baated *et al.,* [23] and meet the minimum requirement of IPC-A standard at 0.089mm for the fillet height at the terminal of the component with IMC layer formed between the copper pad and solder fillet.

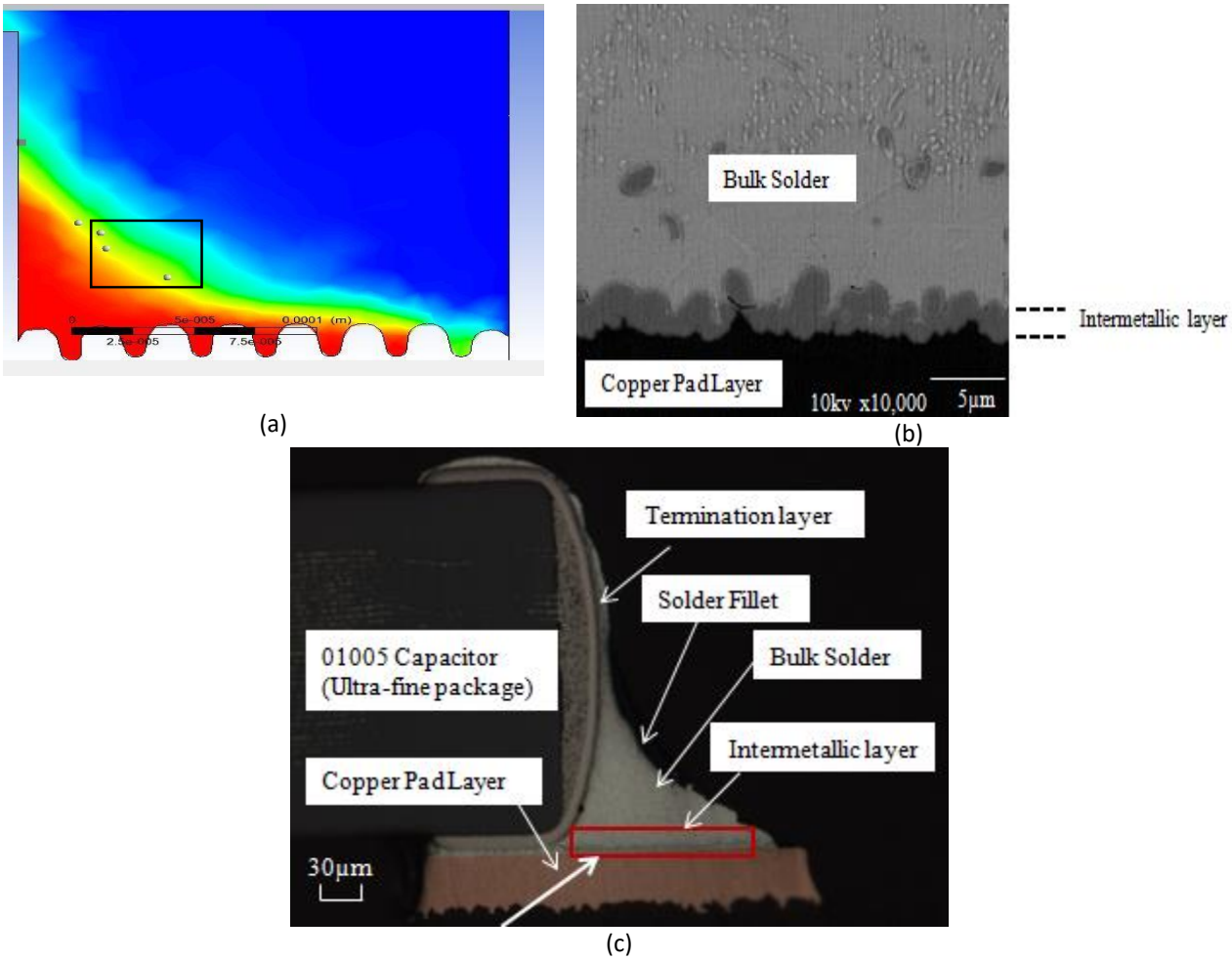

Fig. 6 (a) Fillet observation from the study (b) IMC layer measurement region (c) IMC layer with solder fillet [23]

3.2 Nanoparticles Distribution

Table 5 and Table 6 shows 2D view of the cross-sectioned view of the model VOF solution solder flow with distributed nano-particles weight percentages of 0.01%, 0.15% and 0.15% at different peak temperature. The study is subdivided into two region or phase; soaking and wetting region.

3.3 Soaking and Wetting Region

From the Table 5, there are slight differences exist on the nano-particles distributions due to the effect of changing the peak temperature on the soaking region. The nanoparticles trajectory motions are expected to be dispersed randomly at lower temperature due to the very low Stoke's number of less than 1 [24]. The nanoparticles and the molten solder move simultaneously to the terminal of the 01005 capacitor and the base terminal of the PCB board due to the wetting mechanism. Since the weight percentage and the size of nanoparticles that are very small in molten solder, the momentum and kinetic energy are found to be insignificant [25].

Based on the observations of Table 5 and Table 6, comparing the nanoparticles distributions to each increasing temperature, the nanoparticles seem to be accumulated towards each other at lower temperature and they tend to be evenly distributed at the higher position of the molten solder fillet at higher temperature. This is identified to be the result of nanoparticles' buoyancy effect towards

the molten solder [26]. Generally, buoyancy effect happens when the density of molten solder is higher than of nanoparticles. Hence, higher temperature drops the density of the molten solder and tends to make the nanoparticles to float. Based on the observations, the nanoparticles are in sufficient distant from the IMC layer. This is desirable properties as if there is any particle residing near to the IMC layer, it could damage the solder. Additionally, a distributed nanoparticle gives higher strength of the solder.

Table 5
Nanoparticles distribution during soaking zone

Peak Temperature	0.01%	0.05%	0.15%
175 °C	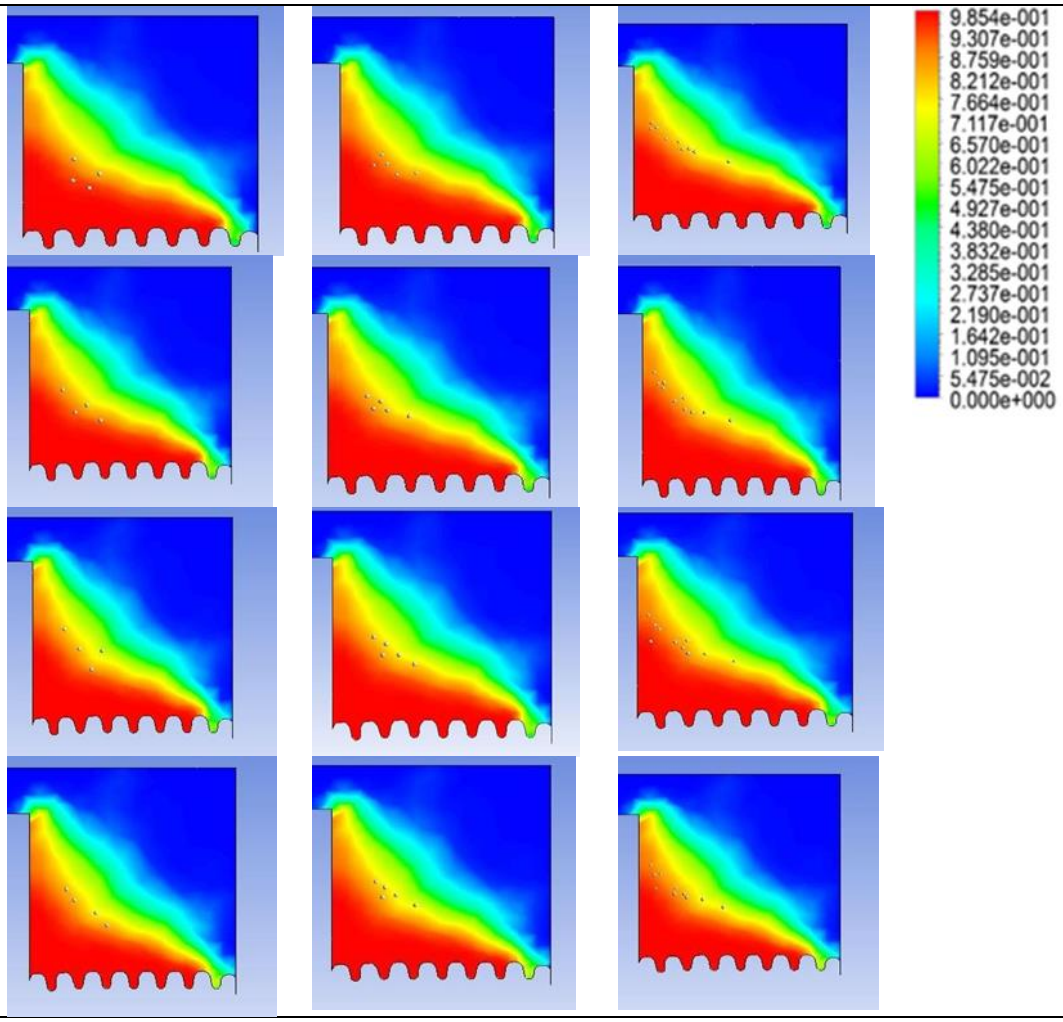		
180 °C			
190 °C			
200 °C			

Table 6
Nanoparticles distribution during wetting region

Peak Temperature	0.01%	0.05%	0.15%
240°C	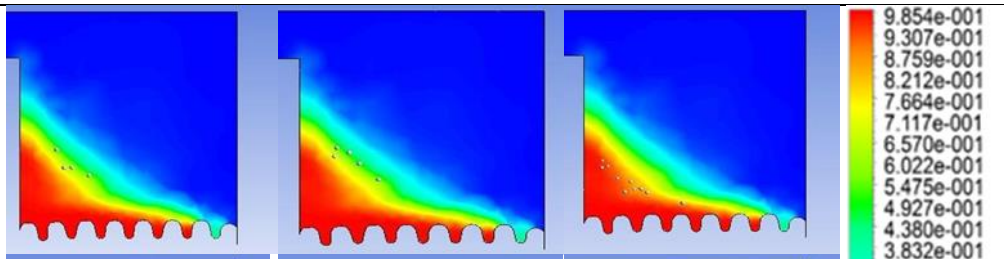		
245°C	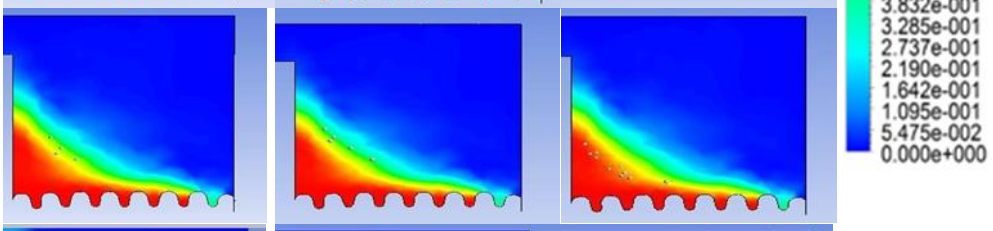		
250°C	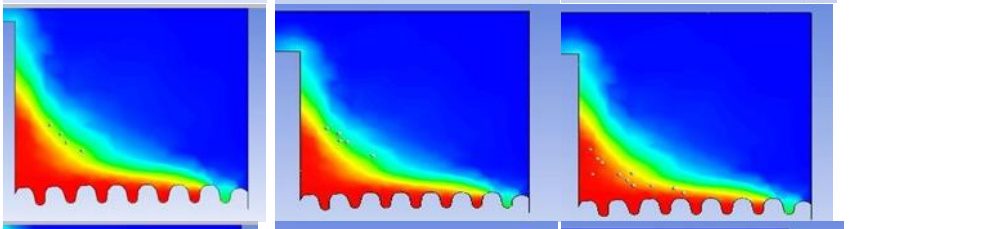		
255°C	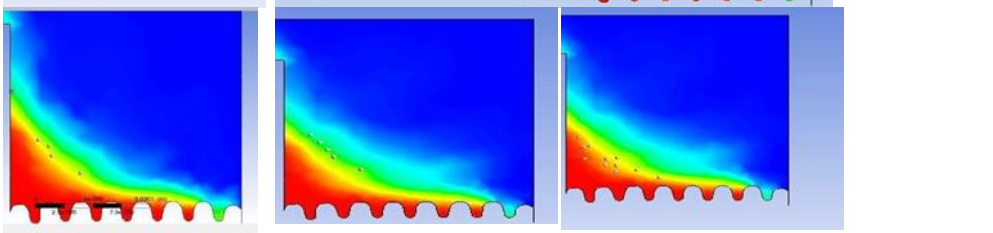		

4. Conclusions

This study has successfully described the effect of peak temperature of wetting region at different value such 240 °C, 245 °C, 250°C and 255°C on the fillet height. These peak temperatures of wetting region are used on a 3D model of ultra-fine package specifically 01005 capacitor. This study concludes that the best fillet height would be obtained at 250°C. This is very crucial to get a suitable fillet height to maintain the solder's strength with minimum formation of IMC layer. The distributions of nanoparticles with 0.01 wt%, 0.05 wt%, and 0.15 wt% of weighted percentage are effectively observed by using the HRTEM analysis. Based on the study, higher temperature of the wetting region that range between 240°C and 255°C results in better particle distributions, and fillet height of the solder by using temperature in that range meets the requirement of IPC standards. This demonstrates that the experimental and simulation results are aligning with each other. This paper has excellently shown the effectiveness of two-way interaction between DPM and VOF models in the means of foreseeing the distribution of nanoparticles in the passive device soldering process.

Acknowledgement
This work was partly supported by the FRGS grant FRGS/1/2015/TK03/USM/03/2 and USM Research University Grant 8014071 from the Division of Research and Innovation, University Sains Malaysia, Engineering Campus, Penang and DRB-HICOM University of Automotive Malaysia, IRGS/012017/004.

References

[1] Abtew, Mulugeta, and Guna Selvaduray. "Lead-free solders in microelectronics." *Materials Science and Engineering: R: Reports* 27, no. 5-6 (2000): 95-141. https://doi.org/10.1016/S0927-796X(00)00010-3

[2] Chang, S. Y., C. C. Jain, T. H. Chuang, L. P. Feng, and L. C. Tsao. "Effect of addition of TiO2 nanoparticles on the microstructure, microhardness and interfacial reactions of Sn3. 5AgXCu solder." *Materials & Design* 32, no. 10 (2011): 4720-4727. https://doi.org/10.1016/j.matdes.2011.06.044

[3] Haslinda, M. S., Aizat Abas, F. Che Ani, Azman Jalar, A. A. Saad, and Mohd Zulkifly Abdullah. "Discrete phase method particle simulation of ultra-fine package assembly with SAC305-TiO2 nano-reinforced lead free solder at different weighted percentages." *Microelectronics Reliability* 79 (2017): 336-351. https://doi.org/10.1016/j.microrel.2017.07.054

[4] Tsao, L. C., and S. Y. Chang. "Effects of Nano-TiO2 additions on thermal analysis, microstructure and tensile properties of Sn3. 5Ag0. 25Cu solder." *Materials & Design* 31, no. 2 (2010): 990-993. https://doi.org/10.1016/j.matdes.2009.08.008

[5] Tsao, L. C., S. Y. Chang, C. I. Lee, W. H. Sun, and C. H. Huang. "Effects of nano-Al2O3 additions on microstructure development and hardness of Sn3. 5Ag0. 5Cu solder." *Materials & Design* 31, no. 10 (2010): 4831-4835. https://doi.org/10.1016/j.matdes.2010.04.033

[6] Chellvarajoo, Srivalli, M. Z. Abdullah, and Z. Samsudin. "Effects of Fe2NiO4 nanoparticles addition into lead free Sn–3.0 Ag–0.5 Cu solder pastes on microstructure and mechanical properties after reflow soldering process." *Materials & Design* 67 (2015): 197-208. https://doi.org/10.1016/j.matdes.2014.11.025

[7] Chellvarajoo, Srivalli, and M. Z. Abdullah. "Microstructure and mechanical properties of Pb-free Sn–3.0 Ag–0.5 Cu solder pastes added with NiO nanoparticles after reflow soldering process." *Materials & Design* 90 (2016): 499-507. https://doi.org/10.1016/j.matdes.2015.10.142

[8] Liu, Lie, Sung Yi, Lin Seng Ong, Kerm Sin Chian, Stephen Osiyemi, Sin Heng Lim, and Fei Su. "Chemothermal modeling and finite-element analysis for microwave cure process of underfill in flip-chip packaging." *IEEE transactions on electronics packaging manufacturing* 28, no. 4 (2005): 355-363. https://doi.org/10.1109/TEPM.2005.857676

[9] Thiruvengadam, Magesh, Yi Zheng, and Jerry C. Tien. "DPM simulation in an underground entry: Comparison between particle and species models." *International Journal of Mining Science and Technology* 26, no. 3 (2016): 487-494. https://doi.org/10.1016/j.ijmst.2016.02.018

[10] Rashidi, Saman, Masoud Bovand, Javad Abolfazli Esfahani, and Goodarz Ahmadi. "Discrete particle model for convective AL2O3–water nanofluid around a triangular obstacle." *Applied Thermal Engineering* 100 (2016): 39-54. https://doi.org/10.1016/j.applthermaleng.2016.01.076

[11] Ho, Jungseok, and Wonil Kim. "Discrete phase modeling study for particle motion in storm water retention." *KSCE Journal of Civil Engineering* 16, no. 6 (2012): 1071-1078. https://doi.org/10.1007/s12205-012-1304-3

[12] Lin, Shanjun, Lu Ding, Zhijie Zhou, and Guangsuo Yu. "Discrete model for simulation of char particle gasification with structure evolution." *Fuel* 186 (2016): 656-664. https://doi.org/10.1016/j.fuel.2016.09.011

[13] Lu, Liqiang, Ji Xu, Wei Ge, Guoxian Gao, Yong Jiang, Mingcan Zhao, Xinhua Liu, and Jinghai Li. "Computer virtual experiment on fluidized beds using a coarse-grained discrete particle method—EMMS-DPM." *Chemical Engineering Science* 155 (2016): 314-337. https://doi.org/10.1016/j.ces.2016.08.013

[14] Tsao, L. C., C. H. Huang, C. H. Chung, and R. S. Chen. "Influence of TiO2 nanoparticles addition on the microstructural and mechanical properties of Sn0. 7Cu nano-composite solder." *Materials Science and Engineering: A* 545 (2012): 194-200. https://doi.org/10.1016/j.msea.2012.03.025

[15] Hongwu, Zhang, Zhao Tianhao, Liu Yang, and Sun Fenglian. "Effect of temperature on failure mode of solder joint under vibration loading condition." In *2013 14th International Conference on Electronic Packaging Technology*, pp. 853-856. IEEE, 2013. https://doi.org/10.1109/ICEPT.2013.6756597

[16] Cheng, Shunfeng, Chien-Ming Huang, and Michael Pecht. "A review of lead-free solders for electronics applications." *Microelectronics Reliability* 75 (2017): 77-95.

https://doi.org/10.1016/j.microrel.2017.06.016

[17] Mukhtar, MA Fatah M., A. Abas, M. S. Haslinda, F. Che Ani, A. Jalar, A. A. Saad, M. Z. Abdullah, and R. Ismail. "Effect of Different S AC Based Nanoparticles Types on the Reflow Soldering Process of Miniaturized Component using Discrete Phase Model Simulation." *Journal of Applied Fluid Mechanics* 12, no. 5 (2019): 1683-1696. https://doi.org/10.29252/jafm.12.05.29553

[18] Mohd Syakirin Rusdi, Mohd Zulkifly Abdullah, Mohd Sharizal Abdul Aziz, Muhammad Khalil Abdullah@Harun, Srivalli Chellvarajoo, Azmi Husin, Parimalam Rethinasamy, and Sivakumar Veerasamy. "Multiphase flow in solder paste stencil printing process using CFD approach." *Journal of Advanced Research in Fluid Mechanics and Thermal Sciences* 46, no. 1 (2018): 147-152.

[19] Wakeman, T., and W. Tabakoff. "Measured particle rebound characteristics useful for erosion prediction." In *Turbo Expo: Power for Land, Sea, and Air*, vol. 79580, p. V003T05A005. American Society of Mechanical Engineers, 1982.

[20] Chan, Yan Cheong, and Dan Yang. "Failure mechanisms of solder interconnects under current stressing in advanced electronic packages." *Progress in Materials Science* 55, no. 5 (2010): 428-475. https://doi.org/10.1016/j.pmatsci.2010.01.001

[21] Ng, Fei Chong, Aizat Abas, Z. L. Gan, Mohd Zulkifly Abdullah, F. Che Ani, and M. Yusuf Tura Ali. "Discrete phase method study of ball grid array underfill process using nano-silica filler-reinforced composite-encapsulant with varying filler loadings." *Microelectronics Reliability* 72 (2017): 45-64. https://doi.org/10.1016/j.microrel.2017.03.034

[22] Fima, Przemyslaw, Tomasz Gancarz, Janusz Pstrus, Krystyna Bukat, and Janusz Sitek. "Thermophysical properties and wetting behavior on Cu of selected SAC alloys." *Soldering & surface mount technology* (2012). https://doi.org/10.1108/09540911211214640

[23] Baated, Alongheng, Junxiang Jiang, Keun-Soo Kim, Katsuaki Suganuma, Sharon Huang, Benjamin Jurcik, Shigeyoshi Nozawa, and Minoru Ueshima. "Sn–Ag–Cu soldering reliability as influenced by process atmosphere." *IEEE transactions on electronics packaging manufacturing* 33, no. 1 (2009): 38-43. https://doi.org/10.1109/TEPM.2009.2035442

[24] Ani, Fakhrozi Che, Azman Jalar, Abdullah Aziz Saad, Chu Yee Khor, Roslina Ismail, Zuraihana Bachok, Mohamad Aizat Abas, and Norinsan Kamil Othman. "SAC–xTiO2 nano-reinforced lead-free solder joint characterizations in ultra-fine package assembly." *Soldering & Surface Mount Technology* 30, no. 1 (2018): 1-13. https://doi.org/10.1108/SSMT-04-2017-0011

[25] Chen, Si, Lili Zhang, Johan Liu, Yulai Gao, and Qijie Zhai. "A reliability study of nanoparticles reinforced composite lead-free solder." *Materials transactions* 51, no. 10 (2010): 1720-1726. https://doi.org/10.2320/matertrans.MJ201002

[26] Ani, F. Che, Azman Jalar, Abdullah Aziz Saad, C. Y. Khor, R. Ismail, Z. Bachok, M. A. Abas, and N. K. Othman. "The influence of Fe 2 O 3 nano-reinforced SAC lead-free solder in the ultra-fine electronics assembly." *The International Journal of Advanced Manufacturing Technology* 96, no. 1-4 (2018): 717-733. https://doi.org/10.1007/s00170-018-1583-z